Rapid translocation of nanoparticles from the lung airspaces to the body

Published in final edited form as:
Nat Biotechnol. 2010 December ; 28(12): 1300–1303. doi:10.1038/nbt.1696.

Rapid Translocation of Nanoparticles from the Lung Airspaces to the Body

Hak Soo Choi[1], **Yoshitomo Ashitate**[1], **Jeong Heon Lee**[1], **Soon Hee Kim**[1], **Aya Matsui**[1], **Numpon Insin**[2], **Moungi G. Bawendi**[2], **Manuela Semmler-Behnke**[3], **John V. Frangioni**[1,4,*], and **Akira Tsuda**[5,*]

[1]Division of Hematology/Oncology, Department of Medicine Beth Israel Deaconess Medical Center, Boston, MA 02215

[2]Department of Chemistry, Massachusetts Institute of Technology, Cambridge, MA 02139

[3]Institute of Lung Biology and Disease, Helmholtz Center München - German Research Center for Environmental Health, Neuherberg/Munich 85764, Germany

[4]Department of Radiology, Beth Israel Deaconess Medical Center, Boston, MA 02215

[5]Molecular and Integrative Physiological Sciences, Harvard School of Public Health, Boston, MA 02115

SUMMARY

Nanoparticles (NPs) have the potential to revolutionize drug delivery, however, administering them to the human body without the need for intravenous injection remains a major challenge. In this study, a series of near-infrared (NIR) fluorescent NPs were systematically varied in chemical composition, shape, size, and surface charge, and their biodistribution and elimination were quantified in rat models after lung instillation. We demonstrate that NPs with hydrodynamic diameter (HD) less than ≈ 34 nm and a non-cationic surface charge translocate rapidly from lung to mediastinal lymph nodes. NPs of HD < 6 nm can traffic rapidly from the lungs to lymph nodes and the bloodstream, and then be subsequently cleared by the kidneys. We discuss the importance of these findings to drug delivery, air pollution, and carcinogenesis.

Keywords

Nanoparticles; nanomedicine; drug delivery; air pollution; lymph node uptake; biodistribution; renal clearance

[*]**Co-Senior Authors:** Beth Israel Deaconess Medical Center 330 Brookline Avenue, Room SL-B05 Boston, MA 02215 Phone: 617-667-0692 Fax: 617-667-0981 jfrangio@bidmc.harvard.edu Harvard School of Public Health 665 Huntington Avenue Boston, MA 02115 Phone: 617-432-0127 Fax: 617-432-4710 atsuda@hsph.harvard.edu .

AUTHOR CONTRIBUTIONS H.S.C., Y.A., J.H.L., S.H.K., A.M., N.I., and A.T. performed the experiments. H.S.C., M.G.B., M.S.B., A.T., and J.V.F. reviewed, analyzed, and interpreted the data. H.S.C., A.T., and J.V.F. wrote the paper. All authors discussed the results and commented on the manuscript.

COMPETING INTERESTS STATEMENT Dr. Frangioni: All FLARE™ technology is owned by Beth Israel Deaconess Medical Center, a teaching hospital of Harvard Medical School. As inventor, Dr. Frangioni may someday receive royalties if products are commercialized. Dr. Frangioni is the founder and unpaid director of The FLARE Foundation, a non-profit organization focused on promoting the dissemination of medical imaging technology for research and clinical use.
Other Authors: None.

Note: Supplementary Information is available on the Nature Biotechnology website.

Nanoparticles (NPs) have been proposed as diagnostic, therapeutic, and theragnostic agents for a wide variety of human diseases.[1-3] Lung-based drug delivery of NPs is receiving increased attention due to the large surface area available and the minimal anatomical barriers limiting access to the body.[4] In this study, we explore whether it would be possible to administer NPs via the lung, and in so doing, attempt to define the key parameters that mediate lung to body NP translocation and subsequent elimination (i.e., clearance).

Lung-administered NPs also have significant implications for air pollution. Recent toxicological studies have confirmed that nano-sized or ultrafine particles reach deep into the alveolar region of the lungs[5,6] and cause severe inflammation reactions due to their large surface areas per mass.[6] Inhalation of NPs is increasingly recognized as a major cause of adverse health effects, and has especially strong influence on the cardiovascular system and hemostasis, leading to increased cardiovascular morbidity and mortality.[6-8]

The standard approach for studying the translocation of inhaled NPs and ultrafine air pollutants from the lungs to extrapulmonary compartments in animals is to perform post-mortem analysis of tissues after inhalation of carbon-based particles,[9] radiotracers,[10] or neutron-activated metal particles.[11-13] Recently, Moller *et al*. reported that ultrafine NPs could pass from the lungs into bloodstream and extrapulmonary organs in humans.[10] Pulmonary macrophages clearly play a key role in the removal of particles from the alveolar gas exchange surface. Harmsen *et al*. elegantly demonstrated alveolar macrophage-mediated translocation of micrometer-sized particles from the lung surface to the regional tracheobronchial lymph nodes (LNs).[14] However, this macrophage-mediated process takes a relatively long time, from several hours to weeks.[13-15]

In this study, we are interested in much more rapid translocation of NPs (on the order of minutes) from the lungs to the draining LNs, to the bloodstream, and to the rest of body. We systematically varied the chemical composition, size, shape, and surface charge of near-infrared (NIR) fluorescent NPs in order to determine how their physicochemical properties affect trafficking across the alveolar surface barrier into tissue, and once in the tissue, their fate with respect to biodistribution and clearance. Enabling this study is our intraoperative FLARE™ (Fluorescence-Assisted Resection and Exploration) imaging system, which permits two independent channels (700 nm and 800 nm) of NIR fluorescence images to be acquired simultaneously with color video images.[16,17] NIR fluorescence imaging provides several advantages for quantifying the process of NP trafficking including a low autofluorescence background, real-time imaging, real-time overlay with anatomy, and highly sensitive detection of targets several millimeters deep in tissue.[18]

As shown in Table 1, two distinct families of NPs were engineered with varying chemical composition, shape, size, and surface charge (see also Fig. 1a). Inorganic/organic hybrid nanoparticles (INPs) emitted at 800 nm. Quantum dots (QDs) with various core(shell) and organic coating ligands were used to produce a variety of sized and charged INPs (INP1 - INP5). Gel filtration chromatography (GFC) was used to measure the final hydrodynamic diameter (HD), which ranged from 5 to 23 nm in phosphate-buffered saline (PBS) (Supplementary Fig. 2 online). It is important to note that the surface-charged INPs with either carboxylic (INP3 and INP5) or amino (INP4) groups showed high protein adsorption, which contributed to a significant increase in final HD when exposed to 100% serum.[19] To study the effect of surface charge in detail, INP1 and INP2 were engineered to have zwitterionic and polar coatings, respectively, which eliminated serum protein binding and resulted in a constant HD in PBS and serum.[19,20] To engineer INPs over 50 nm in HD, we used silica nanospheres doped with QDs and conjugated NIR fluorophore CW800 on the silica surface (INP6 - INP9). These silica NPs did not associate with serum proteins, thus the original size was maintained after 1 h serum incubation at 37°C. Organic nanoparticles

(ONPs) were designed to emit 700 nm NIR fluorescence, which permitted comparison of the effect of NP chemical composition with 800 nm emitting INPs.

To investigate the role of HD in the translocation of NPs from the lung to extrapulmonary compartments of the body, we systematically increased the size of fluorescent NPs from 5 to 300 nm. As shown in Figure 1b, translocation of INP5 and larger particles was severely restricted over 30 min post-administration, which indicates that the size threshold for rapid translocation of NPs from lungs to LNs corresponds to an HD of < 38 nm in serum. Interestingly, a similar size threshold was found in the ONPs; i.e., between 34 nm (ONP3) and 48 nm (ONP4) in HD, suggesting that the rapid translocation from lungs to mediastinal LNs is primarily governed by the size of NPs, irrespective of chemical composition, shape, and conformational flexibility. For charged NPs, non-specific adsorption of endogenous proteins, mostly albumins, can result in a large increase in final HD by 10 to 50 nm (see Supplementary Fig. 2a online).[19,21]

Below the size threshold of 34 nm, the surface charge of NPs also plays a critical role for rapid translocation from lungs to regional LNs (Fig. 1c). To investigate this effect in detail, zwitterionic (INP1 and ONP1), polar (INP2 and ONP2), anionic (INP3 and ONP3), and cationic (INP4) coatings were introduced to both INPs and ONPs, and the charge effect was compared. First, hydrophilic and neutral organic coatings such as zwitterionic cysteine and polar PEG ligands prevented adsorption of serum proteins[19] and led to rapid translocation of NPs into the mediastinal LNs. Nemmar *et al*. demonstrated the importance of surface properties of NPs in hemostasis inducing effects, such as platelet activation, which may lead to thrombosis.[9] On the other hand, the behavior of highly net charged NPs (charge-to-volume ratio > ±1) was more complicated. Since both anionic and cationic charged molecules quickly adsorb endogenous proteins in the lungs, similar migration results were expected among the batches.[19,21] The translocation behavior of NPs in the alveolar lining fluid was, however, very different. Carboxylic group-modified INP3 was found in the LNs within 30 min post-administration, while no significant translocation was observed for the cationic INP4 (Fig. 1c, bottom), even though they were engineered from the same batch of CdTe(CdSe) nanocrystals. Since it is well known that cationic charged materials can be taken up by cells,[22] sometimes causing acute cytotoxicity, it is likely that cationic particles (INP4) were rapidly taken up by pulmonary macrophage and/or epithelial cells shortly after administration, making them unavailable for translocation to LNs. As cationic NPs remain in pulmonary cells for a long time, they may cause severe lung injury.[23] Our results are also consistent with recent reports on pulmonary drug delivery systems that suggest surface charge is a key factor affecting translocation efficiency.[24]

The majority of the administered NPs in our study remained in the lungs, with small amounts rapidly appearing in the mediastinal LNs within 30 min post-administration. Even more rapid translocation (in minutes) from the site of deposition to LNs was only observed in smaller INPs. In particular, for the smallest NPs (INP1, 5 nm), migration to the mediastinal LNs was very fast (within 3 min), and there was measurable NP accumulation in the kidneys and excretion into urine at 30 min post-administration (Fig. 2a). On the other hand, INP3 (27 nm) showed slower accumulation into LNs (<10 min) and blood (<20 min). As shown in Figure 2b, most of our ultra-small NPs were found in the kidneys, with the smallest ones also found in the urine (Supplementary Fig. 4). Because of the zwitterionic surface coating and small HD,[19,25] there were virtually no NPs trapped in the hepatic clearance route, such as liver, bile, and intestine (Fig. 2b).

To confirm the qualitative observations made using NIR fluorescence, INPs were labeled with ^{99m}Tc-MAS_3 (MAS_3 is *S*-acetylmercaptoacetyltriserine) and experiments repeated to better quantitate NP translocation from the lung airspaces to LN, blood, and eventually

urine. Blood clearance was measured by intermittent sampling of the tail vein. The small molecule sodium pertechnetate (TcO_4^-) was used as a control and showed rapid uptake into blood, consistent with direct translocation through the alveolar air-blood barrier,[10] excretion into urine, and moderate uptake in LNs at 1 h post-instillation (Fig. 2c and Supplementary Fig. 5). On the other hand, INP1 and INP3 appeared in the blood after a short lag, and at concentrations inversely proportional to HD. Since LN uptake of NPs was more pronounced than TcO_4^-, this suggests that there could be another pathway for translocation of NPs from lung airspaces into blood, one involving transient passage through LNs. Our findings are also consistent with the literature showing that large cationic liposomes provide an improved therapeutic window to treat lung epithelium. Interestingly, almost no translocation of INP4 was seen in the LNs or carcass (Fig. 2c and Supplementary Fig. 4).

In this study, we have systematically engineered various NPs to demonstrate the effect of particle characteristics on their ability to translocate from the lungs into the LNs and bloodstream, and on their fate *in vivo*. Although NPs are stable and show a narrow size distribution in PBS, this study suggests that the final HD as measured in serum, along with surface charge, play critical roles in determining the ultimate migration, biodistribution, and clearance of NPs deposited in the lungs. The key findings of our study are: 1) a size threshold of ≈ 34 nm mediates whether there is rapid trans-epithelial translocation of NPs from the alveolar luminal surface into the septal interstitium, followed by quick translocation to the regional draining LNs where further translocation into the bloodstream could occur, 2) below this size threshold of ≈ 34 nm, surface charge is a major factor that mediates translocation, with zwitterionic, anionic, and polar surfaces being permissive, but cationic surfaces being restrictive, and 3) when HD is less than 6 nm and surface charge is zwitterionic, NPs can enter the bloodstream quickly from the alveolar airspaces and can ultimately be cleared from the body via renal filtration. The latter finding represents what we believe to be the first description of a “complete cycle” of trafficking of NPs from the environment (i.e., lung airspaces) through the body and back to the environment (i.e., after excretion into urine).

The implications of these findings for drug delivery, air pollution control, and carcinogenesis are significant. Our results might prove useful to investigators trying to engineer inhaled NP-based drugs. First, the data are consistent with the literature showing that large (>100 nm) cationic liposomes provide an improved therapeutic window to treat lung epithelium. That is, systemic absorption is very low, presumably because these NPs exceed the size and charge thresholds defined above (with whatever systemic absorption observed likely due to liposome instability). Second, and more importantly, engineering NP-based drugs to be zwitterionic and < 6 nm in HD should result in rapid and high levels of drug in the bloodstream after administration, while permitting renal clearance of drug not bound to its target. And finally, non-cationic NPs ≤ 34 nm and ≥ 6 nm should provide high levels of drug to pulmonary LNs, which could be used to delivery antibiotics and anti-inflammatory drugs to treat lung infections, tumor metastases, and inflammatory conditions.

With respect to air pollution and carcinogenesis, our data suggest that non-cationic NPs with a HD in serum ≤ 34 nm are potentially the most dangerous in that they rapidly traverse the epithelial barrier, enter regional LNs, and if ≥ 6 nm are not cleared efficiently by the kidneys. Thus, exposure of internal organs and tissues will be maximal. Chemical strategies that alter the size and charge of pollutants to be large (> 34 nm) and cationic could potentially minimize airspace to body translocation, and provide time for macrophage-mediated clearance. Once in the body and lodged in LNs (i.e., 6 nm ≤ HD ≤ 34 nm), non-cationic NPs could cause inflammation and/or contribute to carcinogenesis. Smaller NPs, such as those ≈ 5 nm in HD, are even more concerning for carcinogenesis and distal

inflammation because they are capable of traveling from the lung to the bloodstream, and once in the bloodstream, can potentially reach every tissue and organ in the body.[26]

MATERIALS AND METHODS

Synthesis of inorganic/organic nanoparticles (INPs)

CdSe(ZnCdS) nanocrystals were used to produce INP1 and INP2 with cysteine and dihydrolipoic acid (DHLA)-conjugated polyethylene glycol spacer (DHLA-PEG, MW 1 kDa) coating, respectively, via modification of previously reported procedures (see Supplementary Information online).[19,25] 800 nm NIR emitting fluorophore CW800 (LI-COR, Lincoln, NE) was conjugated on the QD surface in PBS, pH 7.8 (labeling ratio ≈1.4). CdTe(ZnS) core(shell) NIR QDs were purchased from Invitrogen (QDot 800 ITK, Carlsbad, CA) with carboxylated PEG (INP3) or amino PEG (INP4) ligand coating.[27] To engineer INP5, α-amino-ω-carboxylate PEG 3.4 kDa (Nektar, San Carlos, CA) was conjugated through conventional EDC chemistry. INP6 to INP9 silica NPs were prepared by incorporating CdSe(ZnS) QDs in the silica shells, and conjugating CW800 fluorophores on the surface of nanospheres to engineer larger sizes of NPs (see Supplementary Information online).[28]

Synthesis of organic nanoparticles (ONPs)

ONP1 was prepared by a reaction of Cy5.5-NHS (Amersham Biosciences, Piscataway, NJ) with human serum albumin (HSA; American Red Cross, Washington, DC) in PBS at pH 7.8, followed by purification by gel filtration chromatography (GFC) using an Econo-Pac P6 cartridge (Bio-Rad, Hercules, CA). The labeling ratio was 2.6, estimated using the extinction coefficients of HSA (ε_{280nm} = 32,900 $M^{-1}cm^{-1}$) and Cy5.5 (ε_{675nm} = 19,000 $M^{-1}cm^{-1}$). ONP2 was obtained by simply mixing two equiv of Cy5.5-NHS with amino mPEG 20 kDa (Nektar, San Carlos, CA) in PBS at pH 7.8, followed by GFC purification (labeling ratio = 1). A size series of nanospheres based on polystyrene and polyacrylate block copolymers (ONP3 - ONP7) were purchased from Phosphorex, Inc. (Fall River, MA) and conjugated covalently to Cy5.5 (5 to 10 fluorophores per mole of polyacrylate) to produce 700 nm NIR fluorescence emission (see Supplementary Information online).

Double-lumen balloon catheter for NP administration into lungs

Administration of NPs into the lung without backflow entering the trachea and obscuring mediastinal LNs imaging was a major challenge. To solve this problem, we developed a custom-built double-lumen balloon catheter that blocked mucociliary flow into the trachea while animals were being ventilated (see Supplementary Fig. 3 online). A custom-made 20 cm double-lumen balloon catheter was developed by Pelham Plastics, Inc. (Pelham, NH) with the following specifications: OD = 1.5 mm; a thru lumen = 0.71 mm for ventilation; a balloon lumen = 0.5 mm; inflation balloon OD = 2.5 mm. The catheter was inserted through a trachea cannula (OD = 2.1 mm, ID = 1.8 mm) into the right mainstem bronchus and the outer balloon was inflated. The inflated balloon remained in position for 1 h to block backflow of deposited NPs. The thru lumen was used for administration of NP solutions deep into the lung followed by a puff of air during an inspiration phase to ensure delivery of a NP bolus deep into the lung. Both side lungs were ventilated for 60 min.

Animal models

All animals were used under the supervision of an approved institutional protocol. 500 to 550 g Sprague-Dawley (SD) male rats from Charles River Laboratories (Wilmington, MA) were anesthetized with 65 mg/kg intraperitoneal pentobarbital, and were mechanically ventilated by tracheostomy using an MRI-1 ventilator (CWE, Inc. Ardmore, PA) at 80

breaths per min using room air. A specially designed double-lumen balloon catheter was placed in the right mainstem bronchus as described above, and a minimal volume (50 - 100 μL) of NP solution (a mixture of 800 nm INPs and/or 700 nm ONPs) in PBS was then administered through the thru lumen into lungs at a dose of 10 pmol/g of animal weight. After each study, animals were euthanized by intraperitoneal injection of 200 mg/kg pentobarbital, a method consistent with the recommendations of the Panel on Euthanasia of the American Veterinary Medical Association.

Real-time intraoperative NIR fluorescence imaging

The dual-channel intraoperative NIR fluorescence imaging system (FLARE™; Fluorescence-Assisted Resection and Exploration) optimized for animal surgery has been described in detail previously.[16,17] Excitation fluence rate for white light, 700 nm NIR excitation light, and 800 nm NIR excitation light were 20,000 lux, 3.5 mW/cm^2, and 10 mW/cm^2, respectively. The translocation of NPs into LNs and bladder was measured using the following method: the fluorescence (Fl) and background (BG) intensity of a region of interest over each organ was quantified using custom FLARE™ software at the following time points - 0, 1, 2, 5, 10, 20, 30, 40, 50, and 60 min. Signal-to-background ratio (SBR), defined as SBR = (Fl – BG)/BG was then plotted as a function of time. For measuring NP concentration in blood, approximately 20 μL of blood was collected from the tail vein using glass capillary tubes, and the SBR was measured over time. At least three animals were analyzed at each time point. Statistical analysis was carried out using the unpaired Student's t-test or one-way analysis of variance (ANOVA). Results were presented as mean ± S.D. and curve fitting was performed using Prism version 4.0a software (GraphPad, San Diego, CA).

^{99m}Tc-labeling of NPs and radioscintigraphic imaging

^{99m}Tc-conjugated NPs were prepared using high-specific-activity *N*-hydroxysuccinimide (NHS) ester of ^{99m}Tc-MAS$_3$ as described previously.[19,20,26] 50 - 100 μL of ^{99m}Tc-conjugated NPs (100 - 300 μCi) were administered intratracheally into SD rats. Sodium pertechnetate (TcO_4^-) was used as a control. Measurement of blood clearance was performed by intermittent sampling of the tail vein. Rats were sacrificed at 1 h post-administration. To measure total urinary excretion, the bladder was removed *en masse* and combined with excreted urine prior to measurement of radioactivity in a dose calibrator. The radioactivity of each resected major organ was measured on a Wallac Wizard (model 1470, Perkin Elmer, Wellesley, MA) 10-detector gamma counter. Gamma radioscintigraphy was performed with a Research Digital Camera (Isocam Technologies, Castana, IA) equipped with a 1/2″ NaI crystal, 86 photomultiplier tubes, and high-resolution (1 mm) lead collimator.

Histological analysis of tissues

Tissues were resected 1 h post-administration, fixed in 10% formalin for 3 h, molded with Tissue-Tek OCT compound (Fisher Scientific, Pittsburgh, PA), and frozen in liquid nitrogen. Frozen sections were cut to a 10 μm thickness and stained with hematoxylin and eosin (Histotec Laboratories). Lung, liver, spleen, kidney, pancreas, intestine, muscle, and LNs were examined by a 4-channel fluorescence microscope. The excitation and emission filters used were 650 ± 22 nm and 710 ± 25 nm for NIR #1, and 760 ± 20 nm and 790 nm longpass for NIR #2, respectively.

Supplementary Material

Refer to Web version on PubMed Central for supplementary material.

Acknowledgments

We thank Rafiou Oketokoun and Sylvain Gioux for help with developing the FLARE™ imaging system, and Elaine P. Lunsford of the Longwood Small Animal Imaging Facility (LSAIF) for assistance with SPECT/CT imaging. The Biophysical Instrumentation Facility for the Study of Complex Macromolecular Systems (NSF-0070319 and NIH GM68762) is gratefully acknowledged. We thank Wenhao Liu and Binil Itty Ipe for providing quantum dots, Lorissa Moffitt for editing, and Linda Keys and Eugenia Trabucchi for administrative support. This work was supported in part by NIH grant HL054885 (AT), HL070542 (AT), HL074022 (AT), and R01-CA-115296 (JVF).

REFERENCES

1. Janib SM, Moses AS, Mackay JA. Imaging and drug delivery using theranostic nanoparticles. Adv Drug Deliv Rev. 2010
2. Zrazhevskiy P, Sena M, Gao X. Designing multifunctional quantum dots for bioimaging, detection, and drug delivery. Chem Soc Rev. 2010
3. Choi HS, Frangioni JV. Nanoparticles for biomedical imaging: Fundamentals of clinical translation. Mol Imaging. 2010 in Press.
4. Courrier HM, Butz N, Vandamme TF. Pulmonary drug delivery systems: recent developments and prospects. Crit Rev Ther Drug Carrier Syst. 2002; 19:425–498. [PubMed: 12661699]
5. Tsuda A, Rogers RA, Hydon PE, Butler JP. Chaotic mixing deep in the lung. Proc Natl Acad Sci U S A. 2002; 99:10173–10178. [PubMed: 12119385]
6. Oberdorster G. Pulmonary effects of inhaled ultrafine particles. Int Arch Occup Environ Health. 2001; 74:1–8. [PubMed: 11196075]
7. Mills NL, et al. Adverse cardiovascular effects of air pollution. Nat Clin Pract Cardiovasc Med. 2009; 6:36–44. [PubMed: 19029991]
8. Wichmann HE, et al. Daily mortality and fine and ultrafine particles in Erfurt, Germany part I: role of particle number and particle mass. Res Rep Health Eff Inst. 2000:5–86. discussion 87-94. [PubMed: 11918089]
9. Nemmar A, et al. Ultrafine particles affect experimental thrombosis in an in vivo hamster model. Am J Respir Crit Care Med. 2002; 166:998–1004. [PubMed: 12359661]
10. Moller W, et al. Deposition, retention, and translocation of ultrafine particles from the central airways and lung periphery. Am J Respir Crit Care Med. 2008; 177:426–432. [PubMed: 17932382]
11. Kreyling WG, et al. Translocation of ultrafine insoluble iridium particles from lung epithelium to extrapulmonary organs is size dependent but very low. J Toxicol Environ Health A. 2002; 65:1513–1530. [PubMed: 12396866]
12. Semmler M, et al. Long-term clearance kinetics of inhaled ultrafine insoluble iridium particles from the rat lung, including transient translocation into secondary organs. Inhal Toxicol. 2004; 16:453–459. [PubMed: 15204761]
13. Semmler-Behnke M, et al. Biodistribution of 1.4- and 18-nm gold particles in rats. Small. 2008; 4:2108–2111. [PubMed: 19031432]
14. Harmsen AG, Muggenburg BA, Snipes MB, Bice DE. The role of macrophages in particle translocation from lungs to lymph nodes. Science. 1985; 230:1277–1280. [PubMed: 4071052]
15. Geiser M, et al. The role of macrophages in the clearance of inhaled ultrafine titanium dioxide particles. Am J Respir Cell Mol Biol. 2008; 38:371–376. [PubMed: 17947511]
16. Gioux S, et al. High-power, computer-controlled, light-emitting diode-based light sources for fluorescence imaging and image-guided surgery. Mol Imaging. 2009; 8:156–165. [PubMed: 19723473]
17. Troyan SL, et al. The FLARE™ intraoperative near-infrared fluorescence imaging system: a first-in-human clinical trial in breast cancer sentinel lymph node mapping. Ann Surg Oncol. 2009; 16:2943–2952. [PubMed: 19582506]
18. Frangioni JV. In vivo near-infrared fluorescence imaging. Curr Opin Chem Biol. 2003; 7:626–634. [PubMed: 14580568]

19. Choi HS, et al. Renal clearance of quantum dots. Nat Biotechnol. 2007; 25:1165–1170. [PubMed: 17891134]
20. Choi HS, et al. Tissue- and organ-selective biodistribution of NIR fluorescent quantum dots. Nano Lett. 2009; 9:2354–2359. [PubMed: 19422261]
21. Burns AA, et al. Fluorescent silica nanoparticles with efficient urinary excretion for nanomedicine. Nano Lett. 2009; 9:442–448. [PubMed: 19099455]
22. Zhang LW, Monteiro-Riviere NA. Mechanisms of quantum dot nanoparticle cellular uptake. Toxicol Sci. 2009; 110:138–155. [PubMed: 19414515]
23. Brown DM, Wilson MR, MacNee W, Stone V, Donaldson K. Size-dependent proinflammatory effects of ultrafine polystyrene particles: a role for surface area and oxidative stress in the enhanced activity of ultrafines. Toxicol Appl Pharmacol. 2001; 175:191–199. [PubMed: 11559017]
24. Duncan R. Polymer conjugates as anticancer nanomedicines. Nat Rev Cancer. 2006; 6:688–701. [PubMed: 16900224]
25. Liu W, et al. Compact cysteine-coated CdSe(ZnCdS) quantum dots for in vivo applications. J Am Chem Soc. 2007; 129:14530–14531. [PubMed: 17983223]
26. Choi HS, et al. Design considerations for tumour-targeted nanoparticles. Nat Nanotechnol. 2010; 5:42–47. [PubMed: 19893516]
27. Kim S, et al. Near-infrared fluorescent type II quantum dots for sentinel lymph node mapping. Nat Biotechnol. 2004; 22:93–97. [PubMed: 14661026]
28. Insin N, et al. Incorporation of iron oxide nanoparticles and quantum dots into silica microspheres. ACS Nano. 2008; 2:197–202. [PubMed: 19206619]

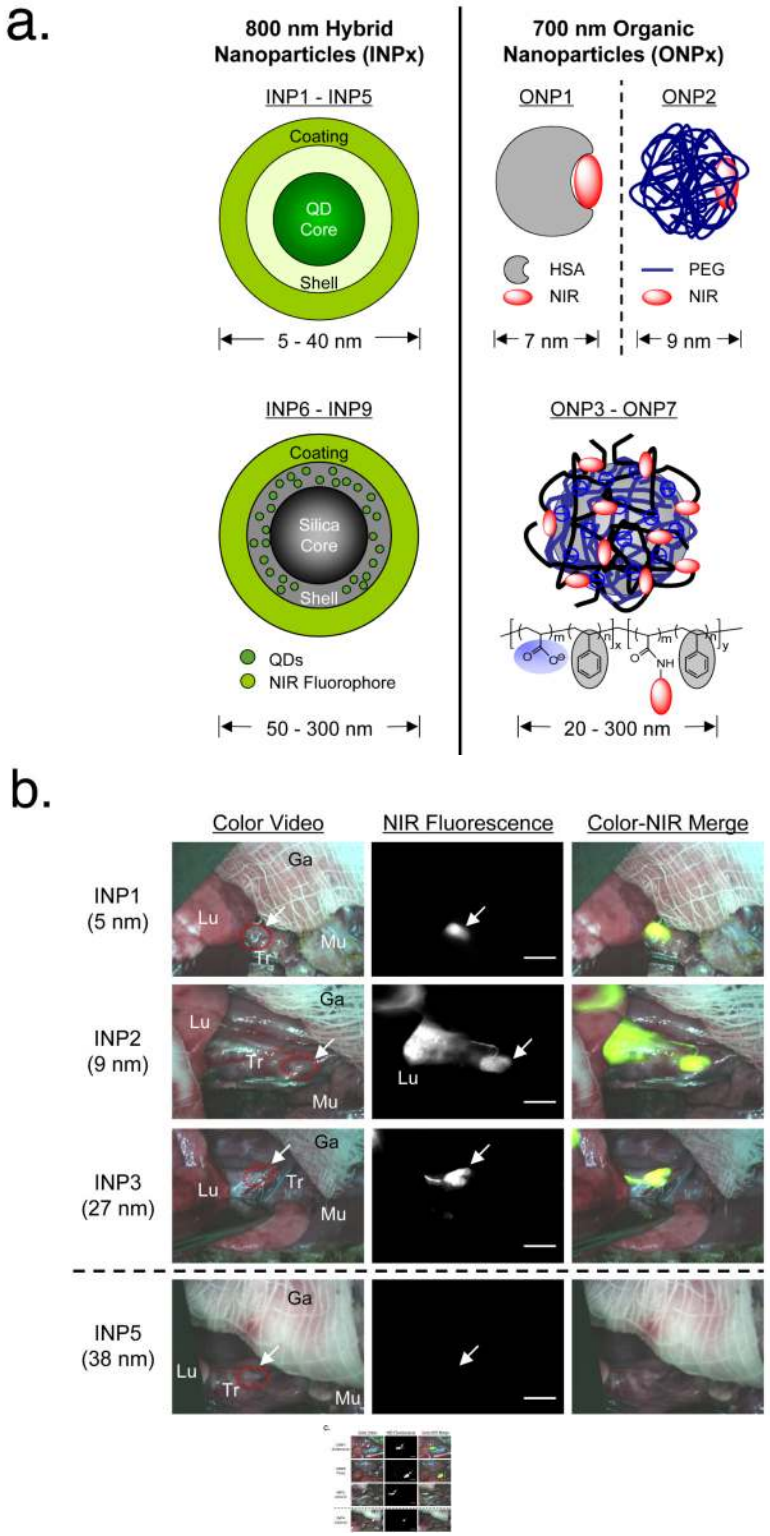

Figure 1.

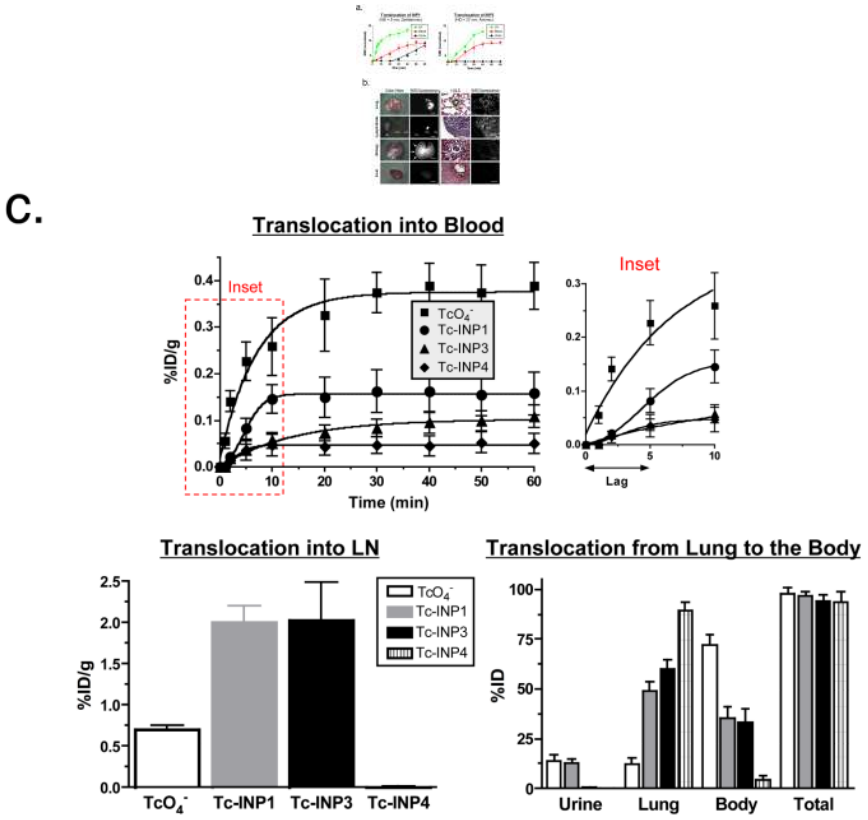

Figure 2.

Table 1

Chemical and physical properties of inorganic/organic hybrid nanoparticles (INPs) and organic nanoparticles (ONPs).

	NP	Core(Shell)	Organic Coating	HD* (nm)		Surface Charge	Emission Max (nm)	Translocation at 1 h	
				in PBS	in Serum			LN (%ID/g)	Non-Lung (Body + Urine; %ID)
Inorganic/Organic Hybrid Nanoparticles (INPs)	INP1	CdSe(ZnCdS)	Cys-CW800	5	5	Zwitterionic	800	2.01	48.1
	INP2	CdSe(ZnCdS)	PEG-CW800	9	9	Polar	800	1.75	35.5
	INP3	CdTe(ZnS)	PEG-COOH	16	27	Anionic	800	2.03	33.8
	INP4	CdTe(ZnS)	PEG-NH2	16	29	Cationic	800	< 0.02	< 5.0
	INP5	CdTe(ZnS)	PEG-COOH	23	38	Anionic	800	0.05	< 5.0
	INP6	Silica/CdSe(ZnS)	CW800	52	56	Polar	800	< 0.02	< 5.0
	INP7	Silica/CdSe(ZnS)	CW800	110	110	Polar	800	< 0.02	< 5.0
	INP8	Silica/CdSe(ZnS)	CW800	130	130	Polar	800	< 0.02	< 5.0
	INP9	Silica/CdSe(ZnS)	CW800	320	320	Polar	800	< 0.02	< 5.0
Organic Nanoparticles (ONPs)	ONP1	HSA	Cy5.5	7	7	Zwitterionic	700	2.18	50.9
	ONP2	mPEG20k	Cy5.5	9	9	Polar	700	1.77†	62.5†
	ONP3	PS-PAA	Cy5.5	21	34	Anionic	700	1.88	42.2
	ONP4	PS-PAA	Cy5.5	35	48	Anionic	700	< 0.02	< 5.0
	ONP5	PS-PAA	Cy5.5	51	68	Anionic	700	< 0.02	< 5.0
	ONP6	PS-PAA	Cy5.5	97	120	Anionic	700	< 0.02	< 5.0
	ONP7	PS-PAA	bCy5.5	220	270	Anionic	700	< 0.02	< 5.0

*HD was measured three times in independent experiments (S.D. ≈ ± 5%) and calculated by the following equation in Prism (an exponential decay equation): $HD = A^{-BX}$, where A = 758.6; B = −0.4709; $R^2 = 0.9951$. Lu = lung and LN = lymph node. Translocation of NPs into LN (%ID/g) and the entire body (except Lu; %ID) was measured at 1 h post-instillation and represents the mean of n = 3 animals except

†n = 2.